Applied Physics A (2021) 127:389
https://doi.org/10.1007/s00339-021-04443-7

Applied Physics A
Materials Science & Processing

T.C. BIOLOGICAL AND BIOMIMETIC MATERIALS

Getting grip in changing environments: the effect of friction anisotropy inversion on robot locomotion

Halvor T. Tramsen[1] · Lars Heepe[1] · Jettanan Homchanthanakul[2] · Florentin Wörgötter[3] · Stanislav N. Gorb[1] · Poramate Manoonpong[2,4]

Received: 3 November 2020 / Accepted: 16 March 2021 / Published online: 29 April 2021

Abstract
Legged locomotion of robots can be greatly improved by bioinspired tribological structures and by applying the principles of computational morphology to achieve fast and energy-efficient walking. In a previous research, we mounted shark skin on the belly of a hexapod robot to show that the passive anisotropic friction properties of this structure enhance locomotion efficiency, resulting in a stronger grip on varying walking surfaces. This study builds upon these results by using a previously investigated sawtooth structure as a model surface on a legged robot to systematically examine the influences of different material and surface properties on the resulting friction coefficients and the walking behavior of the robot. By employing different surfaces and by varying the stiffness and orientation of the anisotropic structures, we conclude that with having prior knowledge about the walking environment in combination with the tribological properties of these structures, we can greatly improve the robot's locomotion efficiency.

Keywords Friction anisotropy · Walking robots · Biomechanics · Asymmetric topography · Stiffness · Computational morphology

1 Introduction

Legged locomotion enables animals to traverse a multitude of different terrains efficiently and quickly. Robotics has mimicked the natural models, creating robots specialized in fast [1, 2] and energy-efficient [3, 4] locomotion with the ability to traverse rough terrain [5, 6] or to move and interact with human environments [7, 8]. Legged locomotion greatly relies on a stable and predictable contact between robot feet and the substrate. Thus, when facing different substrates, the robot has to adapt in order to retain stable and controllable locomotion. This can be achieved either by using feedback control, resulting in great computational cost, or by utilizing computational morphology [9, 10], i.e., specific robot structures and materials facilitating control. Here, by exploiting material and mechanical properties of surface structures for stable surface grip, the morphology of the robot itself can enhance the walking behavior. Many approaches for stable grip employ orientation-dependent anisotropy: a direction dependency of the mechanical properties based on the pulling direction against or along a surface structure on a substrate [11]. A variety of applications employing this concept has been developed such as specific peeling mechanisms of gecko-like adhesives [12, 13], specific gripper movement controls for pipe-climbing robots [14], specific body and leg structures with compliant feet and microstructures [15–17], distributed inward gripping with torsion springs in the foot [18], high-friction rubber on peg legs with multi-step motion planning [19], and even satellite grappling applications in space [20]. Another aspect of orientation-dependent anisotropy has been also studied in active scales which induce frictional anisotropy for efficient snake locomotion (e.g.,

✉ Halvor T. Tramsen
htramsen@zoologie.uni-kiel.de

1 Department of Functional Morphology and Biomechanics, Zoological Institute, Kiel University, Kiel, Germany

2 Bio-Inspired Robotics and Neural Engineering Lab, School of Information Science & Technology, Vidyasirimedhi Institute of Science & Technology, Rayong, Thailand

3 Bernstein Center for Computational Neuroscience (BCCN), The Third Institute of Physics, Georg-August-Universität Göttingen, Göttingen, Germany

4 Embodied AI and Neurorobotics Lab, SDU Biorobotics, The Mærsk Mc-Kinney Møller Institute, University of Southern Denmark, Odense, Denmark

sidewinding and rectilinear locomotion) [21–23]. This active scale-enhanced frictional anisotropy principle has been further explored and applied for locomotion of snake-like robots [24, 25].

To date, many functional surfaces have been investigated and developed, but for mainly one specific task or substrate in mind [15, 26, 27]. However, the world is very diverse, resulting in a multitude of different tasks on a large variety of different substrates, e.g., rigid and compliant ones.

To improve grip and locomote fast and efficiently, we previously investigated a passive anisotropic scale-like material (e.g., shark skin) on different substrates for robot locomotion [28]. The frictional anisotropy of the shark skin's sloped denticles enables the robot to stably grip on the substrate by strong mechanical interlocking in one direction while allowing for an easy release from the substrate in the opposite direction. This way, the robot can efficiently walk on an incline without sliding downward.

In a further study [11], we investigated anisotropic friction properties of a bio-inspired asymmetrically structured sawtooth-like surface as a model anisotropic surface (Fig. 1a). We found that depending on the sawtooth structure and substrate properties, one of two main friction mechanisms dominates friction anisotropy: adhesion-mediated friction or mechanical interlocking. Adhesion-mediated friction, resulting from large contact areas between sawtooth structure and substrate, dominates the friction anisotropy mostly when pulling soft samples along the sawtooth structure on smooth substrates. In contrast, mechanical interlocking is most prominent when pulling rigid sawtooth structures against the sawtooth structure on rougher substrates.

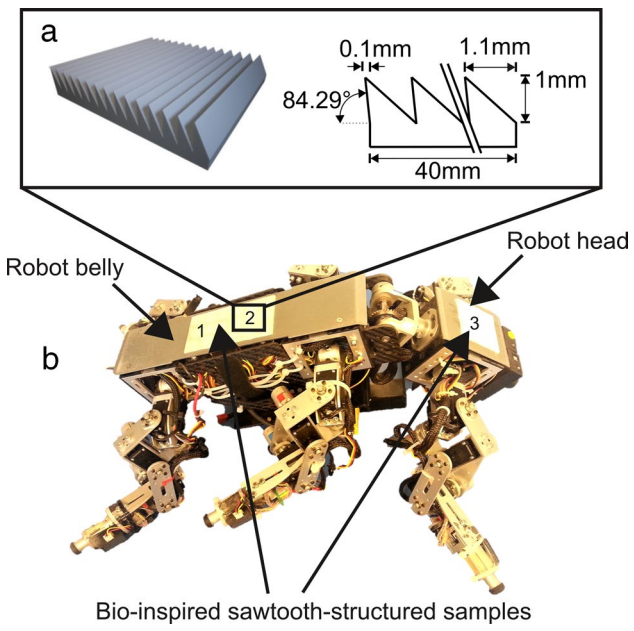

Fig. 1 Anisotropic structures and hexapod walking robot. **a** Profile of the sawtooth structure. **b** Three sawtooth structures installed on the belly and head of the hexapod walking robot AMOSII

This means that friction anisotropy is not solely a result of the anisotropic topography of the structure but can be modified by changing the sawtooth structure stiffness or the substrate roughness, ultimately resulting in a changeover of the dominant friction mechanism. When changing one of these parameters, the anisotropic surface can even exhibit a switching of friction anisotropy, i.e., a complete inversion of the predominant orientation, of a sawtooth-structured surface [11].

In this work, we systematically investigate how attaching the anisotropic model sawtooth structure [11] to a hexapod robot [28] (see Fig. 1b) influences its walking efficiency and speed on various substrates depending on the sawtooth structure orientation. Furthermore, we can show that the inversion of friction anisotropy also occurs in real-life environments when walking over different substrates or when changing the walking direction.

We employ two different stiffnesses for the sawtooth structures, one rigid (Young's moduli of order 1-10GPa) and one soft rubber-like (Young's modulus of order 1 MPa). By attaching them to the robot's belly, we perform static tests to determine the slipping angle of the system on three different substrates. Also, we perform dynamic tests where the locomotion performance of the robot with the anisotropic structures attached is evaluated on the same substrates. This enables us to understand the effect of anisotropic structures for faster and more efficient grip and locomotion of the hexapod robot.

2 Materials and methods

2.1 Sawtooth structure preparation

The sawtooth structures were prepared as described in [11] by molding a metal template in two different stiffnesses. The metal template was produced by wirecutting a metal plate (40 mm x 40 mm x 3 mm) according to the profile shown in Fig. 1a. The soft sawtooth structure was cast from the metal template with polydimethylsiloxane (PDMS: Sylgard 184 [Dow Corning Corp., Midland, MI, USA]) with a Young's modulus of around 2 MPa [29]. The rigid sawtooth structures were molded from such soft sawtooth structures, which had been produced additionally and were not used further for friction measurements, with epoxy resin (Araldite AW 106 resin and HV953 Hardener [Vantico Pty. Ltd, Hongkong, China]) with a Young's modulus of about 5 GPa [30].

2.2 Bio-inspired walking machine

The walking machine AMOSII used in this study is a biologically inspired hexapod hardware platform. Each of its six identical legs (Fig. 1b) has three joints (three degrees of freedom). The thoracocoxal (TC-) joint connects the thorax (main structure/body/head) and the coxa (the first segment of the leg) and enables forward (+) and backward (-) movements. The coxotrochanteral (CTr-) joint connects the coxa and the trochanter (the small second segment of the leg) with the femur (the third segment of the leg) and enables elevation (+) and depression (-) of the leg. The femoro-tibial (FTi-) joint connects the trochanter with the femur and the tibia (the fourth segment of the leg), enabling extension (+) and flexion (-) of the tibia. The morphology of this multi-jointed leg is modeled on an insect leg but the segmented tarsus (foot) is ignored. In insects, the tarsus or foot is the final or distal part of the leg. It typically consists of five segments with one or two claws at the last segment. Here, we use simple rubber semicircle feet instead. The robot body consists of two segments: a front segment (i.e., head) where two front legs are installed and a central body segment (i.e., belly) where the two middle and the two hind legs are attached. They are connected by one active backbone joint. This backbone joint can lean the head segment upward and bend it downward for climbing over an obstacle [31] while during walking it stays at zero degree. In total, the robot has 19 active joints (three joints at each leg, one backbone joint). They are driven by digital servomotors (HSR-5990 TG). Besides the motors, the robot has various sensors to monitor the robot's state and generate stimulus-induced behavior (e.g., phototropism and obstacle avoidance) [32]. A Multi-Servo IO-Board (MBoard) to digitize all sensory input signals and generate a pulse-width-modulated signal to control servomotor position is used. For the robot walking experiments here, the MBoard was connected to a personal computer on which the robot controller was implemented. The update frequency was 25 Hz. Electrical power supply was provided by batteries: one 11.1 V lithium polymer 3200 mAh for all servomotors and two 11.1 V lithium polymers 910 mAh for the electronic board (MBoard) and all sensors (for more details see [33]). In this study, the backbone joint of AMOSII was set to zero degree and we used only a current sensor to monitor energy consumption during robot experiments.

2.3 Friction experiments

We conducted static experiments to investigate the friction coefficients of the sawtooth structures when attached to the robot (see Fig. 2), followed by dynamic experiments to investigate the walking efficiency depending on sawtooth structure orientation and sawtooth structure-substrate combination (see Figs. 3, 4). We evaluated walking efficiency by calculating the specific resistance ϵA:

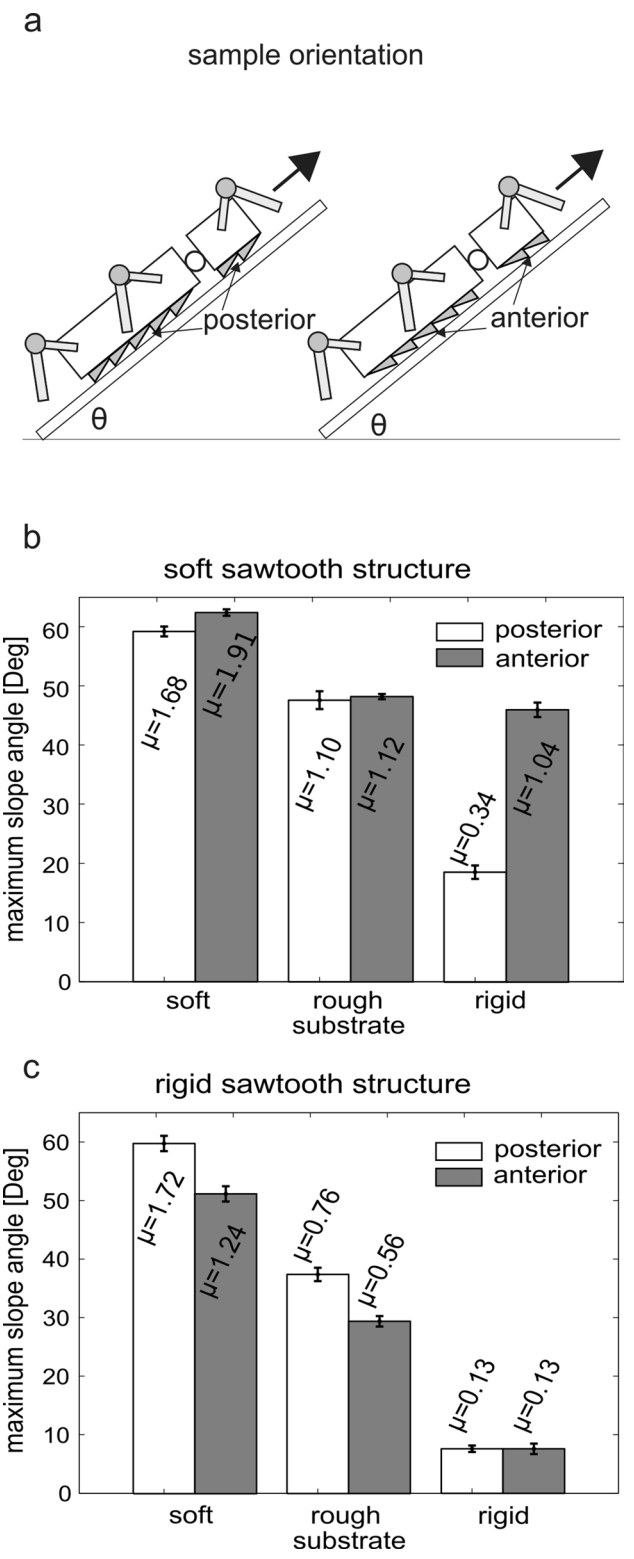

Fig. 2 Static measurements. **a** Sawtooth structure orientations (anterior and posterior) for static and dynamic experiments on an inclined surface with angle θ. **b,c** Maximum angles and calculated friction coefficients of the soft structure **b** and of the rigid structure **c** on all substrates in both sample orientations

$$\varepsilon = \frac{E}{mgd\cos\theta}$$

with the consumed energy E, the weight of AMOSII acting on the substrate mgcos(θ), and the distance traveled d.

Three identical sawtooth structures of either the rigid or the soft material were mounted on the belly of the walking robot AMOSII (with weight of $m = 56.84$ N, as in [28]). The sawtooth structures were either all in posterior or in anterior orientation (see Fig. 2a). The walking experiments were conducted on three different substrates, a rigid substrate (laminated plywood), a soft substrate (foam mat covering the plywood board), and a rough/felt-like substrate (carpet covering the plywood board). See Fig. 3c for pictures of the robot walking on all three different substrates.

2.4 Neural locomotion control

Neural control for locomotion generation of the bio-inspired walking machine AMOSII was previously developed in [33]. The control consists of three main neural networks: Central pattern generator (CPG)-based control network with neuromodulation, neural CPG postprocessing network, and neural motor control network. The CPG-based control network can generate different rhythmic signals for different gaits by setting different values of the neuromodulation parameter. The CPG rhythmic signals are further shaped by the postprocessing network to obtain smooth leg movements. The postprocessed signals are transmitted to all leg joints of AMOSII via the motor control network. The motor control network has two different subnetworks (phase switching network [PSN] and velocity regulating networks [VRNs]) that can regulate the phase and amplitude of the signals for generating different walking directions (i.e., forward, backward and turning). All neurons of the locomotion control network are modeled as discrete-time non-spiking neurons. They are updated with a frequency of approximately 25 Hz. The activity a_i of each neuron develops according to:

$$a_i(t) = \sum_{j=1}^{n} W_{ij}\, o_j(t-1) + B_i, \quad i = 1, ..., n$$

where n denotes the number of units, B_i an internal bias term or a stationary input to neuron i, and W_{ij} the synaptic

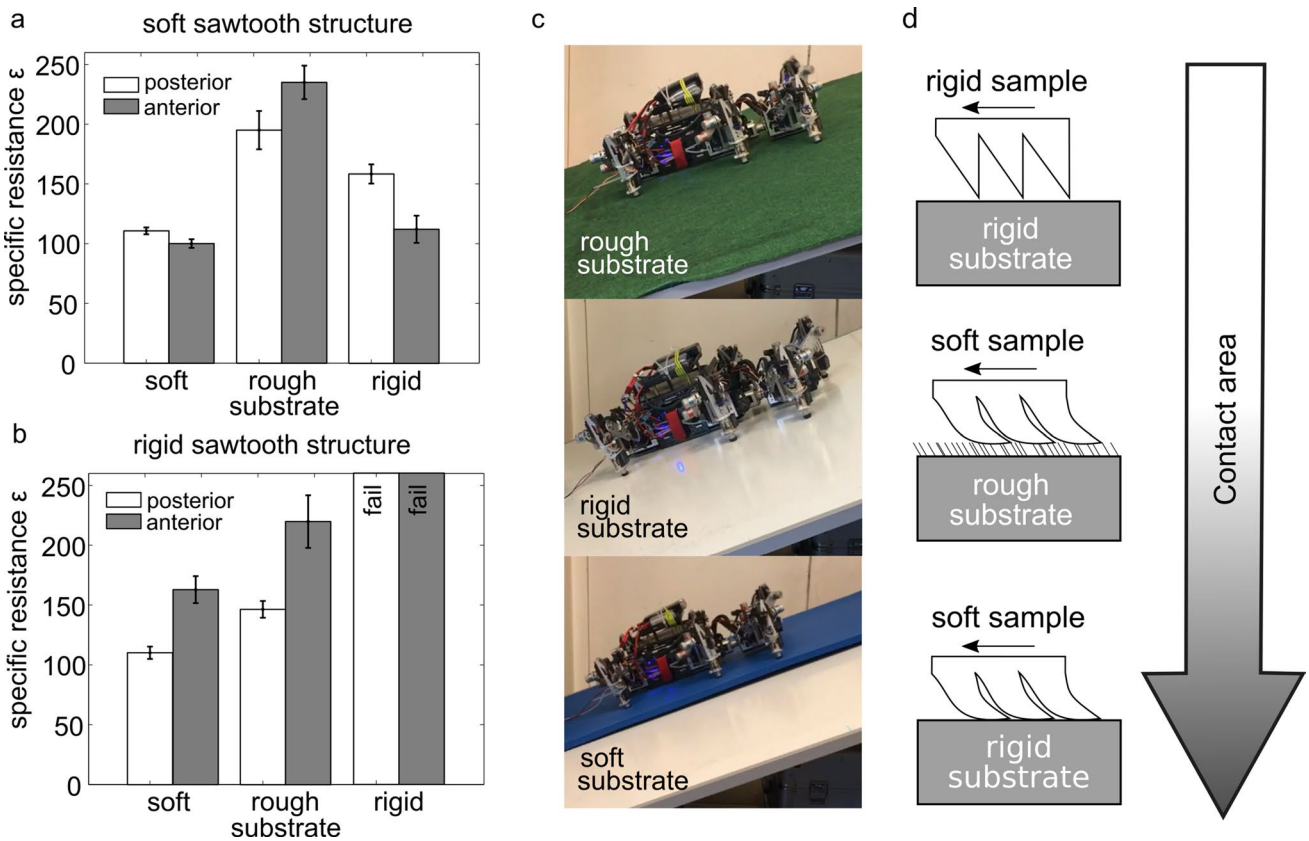

Fig. 3 **a,b** Specific resistance of the soft **a** and the rigid structure **b** on all substrates in both sawtooth structure orientations (anterior and posterior). **c** Hexapod walking robot on all three substrates (rough, rigid and soft). **d** Contact area of sawtooth structure and substrate does not trivially depend on the sawtooth structure and substrate elasticities: the schematic representation exemplarily shows the increase in contact area depending on sawtooth structure elasticity and substrate

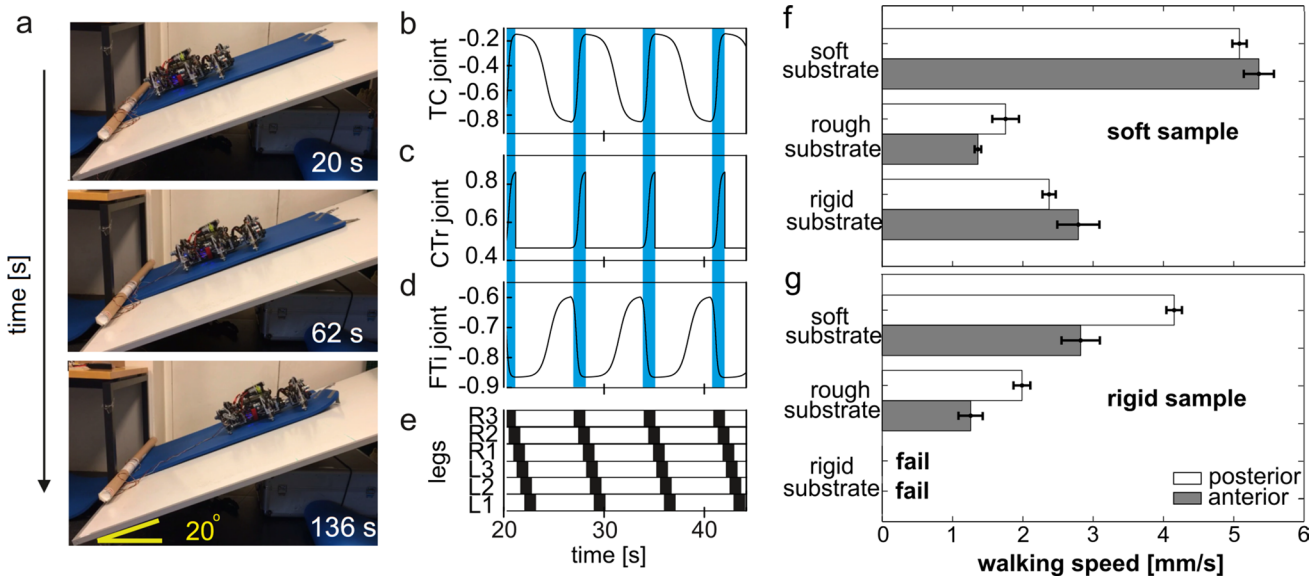

Fig. 4 Dynamic measurements. **a** Experimental setup and snapshots of the experiments at 20, 62 and 136 s with soft substrate, soft sawtooth structure material and anterior sample orientation. **b–d** Example of the motor control signals, which are the outputs of the neural control for controlling robot motor joint positions during walking up the slope with the soft sawtooth structure in anterior orientation on soft substrate (as shown in **a**). Since the neural control used here acts as an open-loop control without sensory feedback and gait adaptation, the motor control signals are also similar in all experimental conditions (i.e. rigid/soft structures, rigid/rough/soft substrate, anterior/posterior orientation). **e** Gait diagram of AMOSII walking up the slope. **f,g** Walking speed on the different substrates **f** for the soft structure and **g** for the rigid structure

strength of the connection from neuron j to neuron i. The output o_i of all neurons of the control network is calculated by using the hyperbolic tangent (tanh) transfer function, i.e., $o_i = \tanh(a_i), \in [-1,1]$, except for the CPG postprocessing neurons using a step function and the motor neurons using piecewise linear transfer functions. The complete description of the locomotion control network can be seen in [33].

In this study, we use the neural locomotion control without any sensory feedback and modification for our robot experiments, i.e., it acts as an open-loop pattern generator. We set the value of the neuromodulation parameter of the control in a way that it generates a slow wave gait for walking up a slope without any gait adaptation (Fig. 4b–e). Thus, the robot uses the same gait in all experiments and the locomotion efficiency is only derived from the contribution of the sawtooth structure material. Using this gait, AMOSII walks with a low center of mass and all the legs swing (off the ground) and stance (on the ground) almost at the same time. As a consequence, the belly of AMOSII touches the ground during the swing phase and stays above the ground with low ground clearance during the stance phase. An advantage of this walking behavior is that AMOSII can rest on its belly during the swing phase. Thus, the motors of the legs do not need to produce high torque to carry the load (i.e., body weight). This also avoids unstable locomotion (i.e., tipping over or falling down).

3 Results

We conducted static experiments to investigate the friction coefficient of the sawtooth structures when attached to the robot (see Fig. 2), followed by dynamic experiments to investigate the walking efficiency depending on sawtooth structure orientation and sawtooth structure-substrate-combination (see Figs. 3, 4).

Three sawtooth-structured samples of one of the two different material stiffnesses were mounted on the belly of the walking robot, all either in posterior or in anterior orientation (see Fig. 2a and Table 1 for an overview of sawtooth structures, orientations and substrates employed).

3.1 Static experiments

To investigate the friction coefficient of the sawtooth structures on different substrates, they were attached to the robot and measured on three types of substrate: rigid, soft, and rough. The static friction coefficient was obtained from the maximum slope angle θ by increasing the slope of the substrate until the robot started sliding downward. For each combination of orientation, sawtooth structure stiffness and substrate, the friction coefficient μ was calculated from this maximum inclination angle θ of the board by $\mu = \tan(\theta)$.

The soft sawtooth structure (see Fig. 2b) generally exhibited higher friction coefficients. Friction anisotropy of the

Table 1 Overview of sawtooth structures, orientations and substrates used in this study

sawtooth structure material:	soft rigid
sawtooth structure orientation:	anterior posterior
substrate:	soft rough rigid

soft structure was mostly observed on the rigid substrate, where the sawtooth structures in anterior orientation exhibited more than twice the friction coefficient of the posterior orientation.

For the rigid sawtooth structure (results are shown in Fig. 2c), the highest friction is also generated on the soft substrate, the lowest friction on the rigid substrate. However, in contrast to the soft sawtooth structure, friction anisotropy is much more pronounced on the soft and rough substrates, while no anisotropy was observed on the rigid substrate.

The inversion of friction anisotropy represents the change in the predominant direction of motion. This can be observed when changing the elasticity of the sawtooth structure on the soft substrate (see Fig. 2b, c). For the soft sawtooth structure, orientation in anterior position yields the highest friction value; however, for the rigid sawtooth structure, highest friction is observed for the posterior orientation.

This effect comes from the change in the dominant friction mechanism from contact area (adhesion)-mediated friction [34, 35] to mechanical interlocking [36–40]. Due to the different degrees of mechanical deformation of the sawtooth structures, the friction behavior of the soft sawtooth structure is mainly dominated by contact area-mediated friction when pulled with the sawtooth structure (anterior orientation), while the rigid sawtooth structure exhibits strong mechanical interlocking on all but the flat rigid substrate when pulled against the sawtooth structure (posterior orientation). Thus here, the higher friction coefficient depends on the orientation of the sawtooth structures and changes from anterior (soft sawtooth structure) to posterior (rigid sawtooth structure) orientation, the anisotropy of the asymmetric structure inverts depending only on the sawtooth structure stiffness (see Fig. 3d for a schematic representation of the varying contact area for adhesion-mediated friction for different sawtooth structure elasticities and substrates).

3.2 Dynamic experiments

To investigate locomotion efficiency, we measured the power consumption as well as the walking speed when the robot, with the sawtooth structures attached to its belly, climbed up a slope with a fixed angle of $\theta = 20°$. We evaluated walking efficiency by calculating the specific resistance ε. The lower ε, the more efficient the robot's locomotion. During the experiments, the robot walked up the slope in a wave gait, which alternates between the swing phase, in which the body rests on the substrate and the legs are put forward consecutively, and the stance phase, where the body is lifted off the ground and then pushed forward (see Fig. 4b-e). In the swing phase, the anisotropic structures on the belly of the robot need to exhibit high friction forces to prevent the robot from sliding down, while in the stance phase, the sawtooth structures should minimize friction forces when the body is pushed forward since during lifting off the ground and setting down, as well as during pushing forward on hairy or springy substrates, friction needs to be minimal.

We can observe the advantages of our sawtooth structures' anisotropic properties, as determined in the static experiments, for the robot locomotion in all dynamic measurements. Huge disparities in specific resistance ε (see Fig. 3) as well as in the corresponding walking speed (see Fig. 4) [41] are visible depending on the orientation and elasticity of the sawtooth structure and on the substrate. With the soft sawtooth structures attached to the robot (for results see Fig. 3b), the most efficient walking, i.e., the lowest specific resistance ε is achieved on the soft substrate in both sawtooth structure orientations as well as on the rigid substrate with the sawtooth structure in anterior orientation. Anisotropy is less pronounced for the soft substrate but occurs strongly on the rough and rigid substrates. However, the anisotropy differs greatly for these two substrates, as an inversion of friction anisotropy can be observed: On the rough substrate, the posterior sawtooth structure orientation yields a lower specific resistance, while on the rigid and soft substrate, the anterior sawtooth structure orientation yields lower specific resistance.

With the rigid sawtooth structures attached to the robot (see Fig. 3c), posterior sawtooth structure orientation results in a lower specific resistance on the soft and the rough substrates, with the soft substrate exhibiting the lowest specific resistance. Only for the rigid sawtooth structure on the rigid substrate, due to the low friction coefficient of this sawtooth structure-substrate combination, the robot slides down the slope regardless of the sawtooth structure orientation. Thus, high forces against sliding down the slope are needed, while the large differences in specific resistances for all other sawtooth structure-substrate combinations clearly show that low friction coefficients in movement direction of the robot are of huge benefit.

Regarding the walking speed (see Fig. 4f, g), an effect of sawtooth structure orientation and sawtooth structure stiffness can be seen: A change in sawtooth structure orientation results in a 47% increase in walking speed for the rigid sawtooth structure on the soft substrate. By varying the sawtooth

structure stiffness, an 89% increase in walking speed can be achieved for the anterior orientation on the soft substrate.

In general, stronger friction anisotropy was observed for the rigid sawtooth structures. However, they failed on the rigid substrate and performed worse on the soft substrate due to the strong deformation of the substrate and resulting mechanical interlocking with the rigid sawtooth structures, slowing the robot down.

The most effective substrate for robot locomotion, for all sawtooth structure elasticities and orientations, was the soft substrate. While the soft sawtooth structure provided sufficiently good friction to enable locomotion on the rigid substrate, the friction coefficient of the rigid sawtooth structures was too low for locomotion on this substrate. On the rough substrate, both sawtooth structure elasticities showed the worst walking efficiencies, thus showing the importance of the interplay of sawtooth structure and substrate for the friction properties.

A change in substrate material also results in an inversion of friction anisotropy. This previously unobserved effect can be seen for the soft sawtooth structure (see Fig. 4f): On the rough substrate, specific resistance is higher in anterior orientation, while for the other two substrates, specific resistance in posterior orientation is higher. This can be explained by the respective dominant friction mechanisms. On the rigid and soft substrates, friction anisotropy results from high forces in anterior sawtooth structure orientation due to adhesion-mediated friction. On the rough substrate, however, adhesion-mediated friction in anterior position decreases drastically due to the minimal contact area on the very rough felt-like substrate [42]. This is in accordance with the static experiments in Fig. 2b, where friction anisotropy is observed on the soft and on the rigid but not on the rough substrate. Thus, the anisotropic properties of the soft sawtooth structures on the rough substrate observed for the dynamic robot experiments seem to originate from the mechanical deformation of the sawtooth structures during locomotion (e.g., deformation during change between stance and swing phases), which is higher in posterior orientation than in anterior orientation due to the asymmetric shape of the sawtooth structures [43].

4 Conclusion

We could successfully show that using anisotropic structures at the belly of the robot to generate friction can greatly enhance fast and energy-efficient robot locomotion. In accordance with previous work [11], we could show that friction anisotropy is not only determined by the asymmetric topography of the sawtooth structures [43], but that other material properties can also fundamentally influence the friction anisotropy and even invert them. Note that without anisotropic structures attached to the robot's belly, the robot slipped, thereby having difficulty climbing up a slope. In contrast, when using an isotropic high friction sample attached to the robot's belly, it could strongly attach to, e.g., rough substrate, thereby preventing slip but could not move forward since it was almost impossible to release from the substrate (see [28]). However, low friction is needed when the robot moves forward on the steep incline or on even ground. Therefore, anisotropic friction is beneficial for achieving the desired energy-efficient robot locomotion by combining high friction forces for grip with low resistance for forward motion. Anisotropic structures clearly facilitate locomotion, with large differences in locomotion efficiency and walking speed depending on the sawtooth structure orientation, elasticity and on the substrate type. Prior knowledge about the tribological properties of the anisotropic structures on the robot belly in contact with various substrates is absolutely necessary to enable efficient locomotion.

We could show that asymmetrical topographies generating anisotropic friction may behave completely differently depending on their stiffness as well as on the substrate properties, possibly resulting in an inversion of friction anisotropy. Thus exhibiting a preferred sawtooth structure orientation for walking, it could, e.g., be beneficial for the robot to climb an incline backward to exploit the anisotropy of its attachment structures if knowledge about the substrate (e.g., by optic sensors or prior knowledge of the environment) indicates that this direction of locomotion will be more efficient for this specific sawtooth structure-substrate combination.

Additionally, we showed that efficient robot locomotion requires more than simply attaching anisotropic structures to the robot's belly: It is beneficial to investigate the structures' tribological properties in detail, because their anisotropic properties not only depend on their asymmetric topography but on many other factors as well, such as stiffness or aspect ratio (see [11] for further discussion). For a better understanding of the transition from adhesion-mediated friction to mechanical interlocking as the dominant friction mechanisms depending on the structure's elastic modulus as well as geometrical shape in combination with different loading parameters, more research will be conducted. Moreover, it is also necessary to consider the substrates which the robot walks on, because changing the substrate may invert friction anisotropy. It could be beneficial to also investigate the effect of contamination, e.g., by fluids or particles on the robot's locomotion and its complex interplay with anisotropic structures. Since the elastic modulus of the sawtooth structures plays a crucial role for the friction properties as well as for the inversion of friction anisotropy, future experiments could also examine the effect of intermediate moduli values on this tribo-robotic system. Finally, the dynamic movements of

the robot may affect the substrate itself, e.g., by deforming a softer substrate due to the robot's weight, thus influencing the effects of sawtooth structure-substrate interaction.

Funding Open Access funding enabled and organized by Projekt DEAL.

References

1. G. Tao, B. Porr, F. Wörgötter, Fast biped walking with a sensor-driven neuronal controller and real-time online learning. Int. J. Robot. Res. **25**(3), 243–259 (2006)
2. J.G. Cham, J.K. Karpick, M.R. Cutkosky, Stride period adaptation of a biomimetic running hexapod. Int. J. Robot. Res. **23**(2), 141–153 (2004)
3. S. Zenker, E.E Aksoy, D. Goldschmidt et al., Visual terrain classification for selecting energy efficient gaits of a hexapod robot. Adv. Int. Mechatronics (AIM), 2013 IEEE/ASME international conference, pp. 577–584 (2013)
4. S. Seok, A. Wang, M.Y.M. Chuah et al., Design principles for energy-efficient legged locomotion and implementation on the MIT Cheetah robot. IEEE/ASME Trans. Mechatron. **20**(3), 1117–1129 (2015)
5. R.B. McGhee, I.I. Georey, Adaptive locomotion of a multilegged robot over rough terrain. IEEE trans. on systems man, cybernet, **9**(4), 176–182 (1979)
6. M. Raibert, K. Blankespoor, G. Nelson et al., Bigdog, the rough-terrain quadruped robot. IFAC Proc. **41**(2), 10822–10825 (2008)
7. J. Chestnutt, M. Lau, G. Cheung, et al., Footstep planning for the honda asimo humanoid. Robotics and Automation, 2005. ICRA 2005. Proceedings of the 2005 IEEE International Conference on. IEEE (2005)
8. A. Albu-Schäffer, S. Haddadin, C. Ott et al., The DLR lightweight robot: design and control concepts for robots in human environments. Ind. Robot: Int J **34**(5), 376–385 (2007)
9. R. Pfeifer, F. Iida, G. Gomez, Morphological computation for adaptive behavior and cognition. Int. Congr. Ser. **1291**, 22–29 (2006)
10. R. Pfeifer, M. Lungarella, F. Iida, Self-organization, embodiment, and biologically inspired robotics. Science **318**, 1088–1093 (2007)
11. H.T. Tramsen, S.N. Gorb, H. Zhang et al., Inversion of friction anisotropy in a bio-inspired anisotropically structured substrate. J. R. Soc. Interface **15**(138), 20170629 (2018)
12. S. Kim, M. Spenjo, S. Trujillo et al., Smooth vertical substrate climbing with directional adhesion. IEEE Trans. Robot. **24**, 65–74 (2008)
13 K.A. Daltorio, S. Gorb, A. Peressadko et al., *A Robot That Climbs Walls Using Micro-Structured Polymer Feet* (In Proc. of Climbing and Walking Robots, Springer, 2006)
14. D. Voigt, A. Karguth, S. Gorb, Shoe soles for the gripping robot: Searching for polymer-based materials maximising friction. Robot. Auton. Syst. **60**, 1046–1055 (2012)
15. M.J. Spenko, G.C. Haynes, J.A. Saunders, et al., Biologically inspired climbing with a hexapedal robot. J. Field Robot. **25**(4–5), 223–242 (2008)
16. S. Kim, A. Asbeck, M. Cutkosky, et al. Climbing hard walls with compliant microspines. In Proc. of the IEEE Int. Conf. Adv. Robot. (ICAR), pp. 601–606 (2005)
17. H. Marvi, J. Bridges, G. Meyers, et al., Scalybot: A snake-inspired robot with active control of friction. In Proc. Of ASME Dynamic Systems and Control Conf. pp. 443–450 (2011)
18. L.R. Palmer, E.D. Diller, R.D. Quinn, Toward a rapid and robust attachment strategy for vertical climbing. In Proc. of the IEEE Int. Conf. on Robotics and Automation, pp. 2810–2815 (2010)
19. T. Bretl, Motion planning of multi-limbed robots subject to equilibrium constraints: The free-climbing robot problem. Int. J. Robot. Res. **25**, 317–342 (2006)
20. H. Jiang, E.W. Hawkes, C. Fuller et al., A robotic device using gecko-inspired adhesives can grasp and manipulate large objects in microgravity. Sci Rob. **2**(7), eaan4545 (2017)
21. H. Marvi, J.P. Cook, J.L. Streator, D.L. Hu, Snakes move their scales to increase friction. Biotribology **5**, 52–60 (2016)
22. D.L. Hu, J. Nirody, T. Scott, M.J. Shelley, The machanics of slithering locomotion. Proc. Natl. Acad. Sci. U.S.A. **106**, 10081–10085 (2009)
23. H.C. Astley, C. Gong, J. Dai et al., Modulation of orthogonal body waves enables high maneuverability in sidewinding locomotion. Proc Nat. Acad. Sci. **112**(19), 6200–6205 (2015)
24 A. Rafsanjani, Y. Zahngy, B. Liu, S.M. Rubinstein, K. Bertoldi, Kirigami skins make a simple soft actuator crawl. Sci. Robot. **3**(15), eaar7555 (2018)
25. A.H. Chang, P.A. Vela, Shape-centric modeling for control of traveling wave rectilinear locomotion on snake-like robots. Robot. Auton. Syst. **125**, 103406 (2020)
26. R.E. Horchler, R.D. Quinn, K.A. Daltorio, et al., A Robot that Climbs Walls using Micro-structured Polymer Feet. Climbing and Walking Robots: Proceedings of the 8th International Conference on Climbing and Walking Robots and the Support Technologies for Mobile Machines (CLAWAR 2005), Springer (2006)
27. K. Inoue, T. Tsurutani, T. Takubo, et al., Omnidirectional gait of limb mechanism robot hanging from grid-like structure.Intelligent Robots and Systems IEEE/RSJ International Conference on Intelligent Robots and Systems, pp. 1732–1737 (2006)
28. P. Manoonpong, D. Petersen, A. Kovalev et al., Enhanced locomotion efficiency of a bioinspired walking robot using contact substrates with frictional anisotropy. Sci. Rep. **6**, 39455 (2016). https://doi.org/10.1038/srep39455
29. L. Heepe, D.S. Petersen, L. Tölle et al., Sexual dimorphism in the attachment ability of the ladybird beetle *Coccinella septempunctata* on soft substrates. Appl. Phys. A **123**(1), 34 (2017)
30. J.E. Mark (ed.), *Polymer Data Handbook* (Oxford University Press, Oxford, 2009)
31 D. Goldschmidt, F. Wörgötter, P. Manoonpong, Biologically-inspired adaptive obstacle negotiation behavior of hexapod robots. Front. Neurorobot. (2014). https://doi.org/10.3389/fnbot.2014.00003
32. E. Grinke, C. Tetzlaff, F. Wörgötter, et al., Synaptic plasticity in a recurrent neural network for versatile and adaptive behaviors of a walking robot. Front. Neurorobot. **9** (11) (2015)

33. P. Manoonpong, U. Parlitz, F. Wörgötter. Neural control and adaptive neural forward models for insect-like, energy-efficient, and adaptable locomotion of walking machines. Front. in neural circuits 7.12 (2013)
34. B.N.J. Persson, Silicone rubber adhesion and sliding friction. Tribol. Lett. (2016). https://doi.org/10.1007/s11249-016-0680-0
35. R. Heise, V.L. Popov, Adhesive contribution to the coefficient of friction between rough surfaces. Tribol. Lett. **39**, 247–250 (2010). https://doi.org/10.1007/s11249-010-9617-1
36. H. Marvi, D.L. Hu, Friction enhancement in concertina locomotion of snakes. J. R. Soc. Interface **9**, 3067–3080 (2012). https://doi.org/10.1098/rsif.2012.0132
37. M.J. Baum, A.E. Kovalev, J. Michels et al., Anisotropic friction of the ventral scales in the snake *Lampropeltis getula californiae*. Tribol. Lett. **54**, 139–150 (2014). https://doi.org/10.1007/s11249-014-0319-y
38. J.M.R. Bullock, W. Federle, The effect of surface roughness on claw and adhesive hair performance in the dock beetle *Gastrophysa viridula*. Insect Sci. **18**, 298–304 (2011). https://doi.org/10.1111/j.1744-7917.2010.01369.x
39. Y. Song, Z. Dai, Z. Wang et al., The synergy between the insect-inspired claws and adhesive pads increases the attachment ability on various rough surfaces. Sci. Rep. **6**, 26219 (2016). https://doi.org/10.1038/srep26219
40. Z. Dai, S.N. Gorb, U.J. Schwarz, Roughness dependent friction force of the tarsal claw system in the beetle *Pachnoda marginata (Coleoptera, Scarabaeidae)*. J. Exp. Biol. **205**, 2479–2488 (2002)
41. P. Gregorio, M. Ahmadi, M. Buehler, Design, control, and energetics of an electrically actuated legged robot. IEEE Trans. Syst., Man, Cybern., Syst. **27**, 626–634 (1997)
42. B.N.J. Persson, Adhesion between an elastic body and a randomly rough hard surface. Eur. Phys. J. E. **8**(4), 285–401 (2002)
43. Z. Mróz, S. Stupkiewicz, An anisotropic friction and wear model. Int. J. Solids Struct. **31**(8), 1113 (1994)